P.2.29 ESTIMATION OF DUST AEROSOL OPTICAL THICKNESS AND ITS SHORTWAVE RADIATIVE FORCING FROM GOES8 IMAGER

Jun Wang and Sundar A. Christopher
Department of Atmospheric Sciences, University of Alabama in Huntsville, Huntsville, AL, 35805

1. INTRODUCTION

Natural as well as anthropogenic aerosols affect the earth-atmosphere system by direct scattering and absorbing of sunlight and indirectly by modifying the radiative properties of clouds. Dust, which is a common aerosol over the desert, can be transported to downwind areas thousands of miles away from source regions; thereby playing an important role on the regional and global radiative energy balance both at the top of atmosphere (TOA) and at the surface. Aerosol optical thickness (AOT) is an important factor to quantify the aerosol radiative forcing. However, current ground-based observations of AOT are very limited. The AOT retrievals from satellite instruments therefore play a very important role for the description of aerosol distributions and validation of the numerical model results.

Polar-orbiting satellites view the globe on a daily basis and retrievals from these satellites provide valuable information on the geographical distribution of aerosols. However, compared to geostationary satellites that have a high temporal resolution within hours or less, polar-orbiting satellites are limited in their ability to fully capture the diurnal variation of aerosols. In this paper we examine the diurnal variations of dust AOT and its corresponding shortwave (SW) aerosol radiative forcing (SWARF) using geostationary satellite (GOES8) data, ground-based measurements as well as radiative model calculations during the Puerto Rico Dust experiment (PRIDE, 14°N-26°N, 61°W-73°W, June 22 to July 22, 2000) (Reid et al., 2002).

2. DATA AND MODELS

The following data sets and radiative transfer models were used:

- The aerosol scattering and absorption coefficient measured from ground-based Nephelometer; aerosol number size distribution data with time resolution of 20 minutes measured from two ground-based particle sizers covering a size range from 0.003 to 15μm (Savoie et al., 2002).
- AOT inferred from Sun Photometers (SP) over two AERONET (Holben et al., 1998) observation sites, Roosevelt Road (RR, 18.20°N, 65.60°W) and La Paguera (LP, 17.97°N, 67.05°W).
- Downward SW irradiance (DSWI) of direct, diffuse and total components at the surface with time of resolution of 1 minute measured from pyranometers at RR site.
- Half-hourly GOES data from June 28 to July 26, 2000.
- The plane parallel Discrete Ordinate Radiative Transfer (DISORT) model (Ricchiazzi et al., 1998) is used for the creation of lookup table (LUT).
- The four-stream radiative transfer model (Fu and Liou, 1993; hereafter 4S model) is used for flux calculations.

3. METHOD

3.1 *Aerosol Optical Properties*

Aerosol optical properties (AOP) are derived by combined use of measured size distribution, light scattering and absorption coefficients and SP AOTs. The refractive index at 0.5μm is first estimated when the best match between the calculated and measured light scattering and absorption coefficient is found. The SP AOTs are used to derive the extinction cross section curve as a function of different wavelengths. During the calculation of aerosol properties, dust aerosol shape is assumed to be spherical and a qualognormal size distribution derived from the measured mean size distribution is used in the Mie calculations. A refractive index of 1.53-0.0015i provides the best match between calculated and measured absorption coefficient at 0.5μm. Using this refractive index and qualognormal size distributions in Mie calculations, the single scattering albedo of dust aerosols, is about 0.98 and the calculated scattering coefficient has an excellent agreement with measured quantities. The detailed steps and the derived broadband

*Corresponding author address: Jun Wang, Dept. of Atmospheric Sciences, NSSTC, 320 sparkman drive, Huntsville, AL, 35805;
e-mail:wangjun@nsstc.uah.edu

aerosols properties used in this study can be found in Christopher et al (2002) and Wang et al (2002).

3.2 LUT Creation and AOT Retrievals

The AOT retrievals are based on a LUT method. First, the derived aerosol properties are used in the DISORT model to create the LUTs in which the TOA reflectance is calculated as a function of different sun-satellite geometries, AOTs and surface reflectance. Second, clear sky sea surface reflectance at each GOES8 observation time period is inferred by use of minimum composite method (Moulin et al., 1997). Thirdly, a dust detection and cloud mask algorithms based on the multi-channel threshold techniques are developed to judge the non-cloudy pixels. In the end, the dust AOT of each non-cloudy pixel is retrieved by finding the best fit between GOES8 TOA reflectance and pre-calculated TOA reflectance in LUTs.

3.3 Flux and SWARF Calculations

The derived broadband AOP are used in the 4S model for the flux calculations. Other inputs also include AOTs, surface albedo and the vertical profile of temperature, water vapor and pressure. The surface albedo used in study is a function of solar zenith angles (Charlock et al., 1997). The atmosphere profile is inferred from the daily sounding datasets. The background flux is calculated from the 4S model by assuming clear sky AOT as 0.07 (Kaufman et al., 2001; Reid et al., 2002). Thus, for each GOES8 non-cloudy pixel, the SW flux both at the surface and the TOA are calculated. The SWARF at the surface and TOA are then calculated using the following formula:

$$\Delta F^{\downarrow}_{toa} = F^{\downarrow}_{toa,\ dust} - F^{\downarrow}_{toa,\ bg} \qquad (1)$$

$$\Delta F^{\downarrow}_{sfc} = F^{\downarrow}_{sfc,\ dust} - F^{\downarrow}_{sfc,\ bg} \qquad (2)$$

where $F^{\downarrow}$ denotes the net downward flux (downward minus upward flux); the subscripts "toa" and "sfc" denote TOA and the surface; and "dust" and "bg" denotes dusty and background conditions, respectively.

4. RESULTS

4.1 GOES8 AOT vs. AERONET AOT

To validate GOES8 retrievals, the SP AOTs in RR and LP sites are collocated with the GOES8 retrievals by use of an optimum time/space window (i.e., +/- 15 minutes time differed; mean GOES AOTs within a 12kmX12km box). To minimize the coastal effect on the retrievals, the 12kmX12km box is not centered at AERONET sites, but was about 3 GOES8 IR pixels from AERONET sites. Figure 1a and 1b shows a good correlation between GOES8 calculated AOTs and SP AOTs at LP and RR sites, with linear correlation coefficients of 0.80 and 0.91 respectively. The vertical and horizontal error bars in figure 1 denote the standard deviation in space (GOES8 AOTs within 12kmX12km box) and time (SP AOTs within +/- 15 minutes). Also shown in the inset of figure 1a and 1b are the frequency distributions of the SP and GOES8 retrieved AOT for both sites. The mean and standard deviation of GOES8 retrievals on RR and LP in figure 1 are 0.19 ± 0.13 and 0.22 ± 0.12 respectively, showing a very good agreement with result of SP AOTs, 0.23 ± 0.13 and 0.22 ± 0.10.

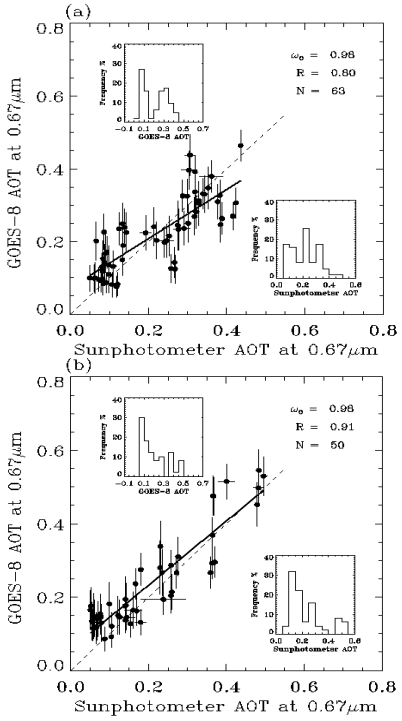

Figure 1. Comparison of GOES8 AOT with SP AOT for LP (a) and RR site (b).

4.2 Calculated DSWI vs. Measured DSWI

To validate the derived broadband aerosol properties and the fluxes calculated from the 4S model, the DSWI from pyranometers is first compared with the calculations. The calculated fluxes are in excellent agreement with measured DSWI components, with linear coefficients of

0.998, 0.9978, and 0.962 for total, direct and diffuse DSWI respectively. Figure 2 shows the comparison of total and direct component respectively. The differences between calculated and measured DSWI are less than 2% that is within the accuracy of instruments and models.

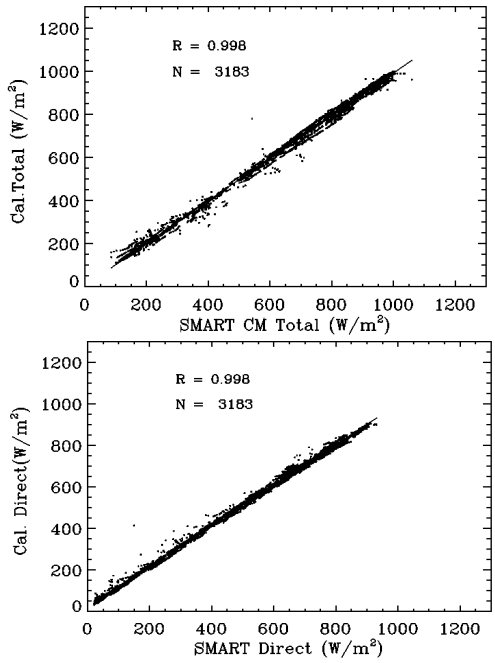

Figure 2. Comparison of calculated and measured DSWI of total (a) and direct (b) components.

4.3 Diurnal SWARF at TOA and Surface

The retrieved GOES8 AOTs with temporal resolution of 30 minutes are then input into the 4S model to calculate the SWARF at the TOA and the surface. Figure 3 (next page) shows an example of the geographic distribution of dust AOTs and their SWARFs on TOA and surface when a dust layer was approaching the Puerto Rico from the Southwest. The GOES8 AOT map during PRIDE period can be found at http://vortex.nsstc.uah.edu/~wangjun/pride/GOES AOT/. Figure 4 shows the monthly mean diurnal SWARF at TOA and surface as well as the corresponding diurnal variations of AOTs in the study area (14°N-26°N, 61°W-73°W). Between 1401UTC to 1631UTC, most of the study area was contaminated by sun glint. Also GOES8 data at 1801 and 1831 UTC was not available in our data archive. Figure 4 shows that the AOT ranges from 0.20 to 0.3, and are quite uniform except during 1701 and 1731 UTC where AOT values are about 0.05 lower than that in other time periods. The monthly mean AOT (0.26) retrieved from GOES8 agrees well with the mean SP derived AOT values of 0.24 and 0.27 at LP and RR sites. The daytime averaged mean SWARF at TOA and surface are –12.34 and –18.31wm^{-2} respectively during PRIDE.

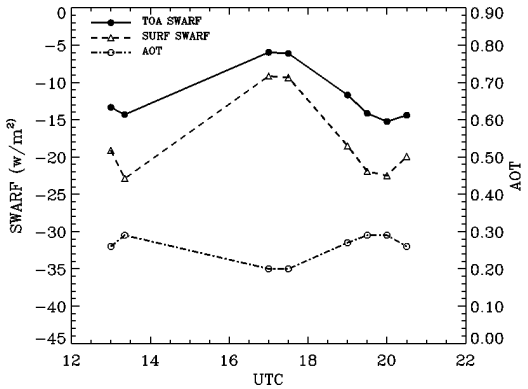

Figure 4. Monthly mean diurnal AOT and SWARF at the TOA and surface during PRIDE.

5. CONCLUSIONS

Our calculated SWARF of dust aerosols at the TOA (–12.34wm^{-2}) in the Puerto Rico region is small when compared with regions with heavy dust loading near source regions such as Africa (e.g., Haywood *et al*, 2001). This is due to the small AOT values in the study area (monthly mean value of 0.26) when compared with AOT values near source regions (a mean AOT value of 0.4 was reported at Cape Verde during PRIDE period *Reid et al.*, 2002).

We then compare our results with previous studies of global mean SWARF both over land and over oceans. Our calculated SWARF is the effect of aerosol in the daytime clear sky conditions. Following the formula by *Charlson et al* (1991), monthly mean daytime "clear sky" SWARF was divided by a factor of 2 (to average both for day and night) and was then multiplied by the clear sky percentage (calculated from GOES8 cloud detection algorithms) to get the regional daily averaged "all sky" monthly mean SWARF that is –4.13Wm^{-2} at TOA and –6.7Wm^{-2} at the surface. When compared to the global mean dust SWARF (–0.062Wm^{-2} ~ –0.25Wm^{-2}, *IPCC,* 2001), the large regional "all sky" SWARF in our studies shows that the dust aerosols in the Puerto Rico region in July has an important contribution to the global dust aerosol forcing. This study shows the potential of geostationary satellite to capture the diurnal variations of AOT as well as SWARF geographic distributions. The algorithms developed as part of this study can be applied to the next generation of geostationary satellites (e.g. Meteosat Second

generation, MSG) to provide accurate estimation of SWARF with high temporal and spatial resolutions.

Reference:

Charlson, R. J., J. Langner, C. B. Leovy, and S. G. Warren, 1991: Perturbation of the Northern Hemisphere radiative balance by backscattering from anthropogenic sulfate aerosols, *Tellus*, **43**AB, 152-163.

Charlock, T. P., F. G. Rose, D. A. Rutan, T. L. Alberta, D. P. Kratz, L. H. Coleman, N. M. Smith, and T. D. Bess, 1997, CERES Algorithm Theoretical Basis Document, subsystem 5.0, Compute Surface and Atmospheric Fluxes. Available at http://eospso.gsfc.nasa.gov/atbd/cerestables.html

Christopher, S. A., J. Wang, Q. Ji, S-C. Tsay, 2002: Estimation of diurnal shortwave dust aerosol radiative forcing during PRIDE, submitted to *J. Geophys. Res.*

Fu, Q., and K. N. Liou, 1993: Parameterization of the radiative properties of cirrus clouds, *J. Atmos. Sci.*, ***50***, 2008-2025.

Haywood., J. M., P .N. Francis, M. D. Glew, and J. P. Taylor, 2001: Optical properties and direct radiative effect of Saharan dust: A case study of two Saharan dust outbreaks using aircraft data, *J. Geophys. Res.* ***106***, 18,417 –18430.

IPCC, 2001: Climate Change 2001: The Scientific Basis. Contribution of Working Group I to the Third Assessment Report of the Intergovernmental Panel on Climate Change, Cambridge University Press, United Kingdom and New York, NY, USA, 881pp.

Kaufman, Y. J., A. Smirnov, B. N. Holben, and O. Dubovik, 2001: Baseline maritime aerosol: methodology to derive the optical thickness and scattering properties, *Geophys. Res. Lett.*, ***28***, 3251-3254.

Moulin, C, H. R. Gordon, V. F. Banzon, and R. H. Evans, 2001: Assessment of Sahara dust absorption in the visible from SeaWiFS imagery, *J. Geophys. Res.* ***106***, *16,*18,239-18,250.

Patterson, E. M., D. A. Gillette, and B. H. Stockton, 1997: Complex index of refraction between 300nm and 700nm for Sahara aerosols, *J. Geophys. Res.*, ***80***, 3153-3160.

Reid, J. S., and coauthors, 2002: Measurements of Saharan dust by airborne and ground-based remote sensing methods during the Puerto Rico Dust Experiment (PRIDE), submitted to *J. Geophys. Res* .

Ricchiazzi, P., S. Yang, C. Gautier, and D. Sowle, 1998: SBDART: A research and teaching software tool for plane-parallel radiative transfer in the Earth's atmosphere, *Bull. Am. Meteorl. Soc.*, ***79***, 2101-2114.

Savoie, D. L., H. B. Maring, and S. A. Christopher, 2002: Spectrally-resolved light absorption by Saharan aerosols over the tropical North Atlantic, submitted to *J. Geophys. Res.*

Wang, J, S. A. Christopher, J. S. Reid, H. Maring, B. N. Holben, and S. K. Yang, 2002: GOES-8 retrieval of dust aerosol optical thickness over the Atlantic ocean during PRIDE, accepted, *J. Geophys. Res.*

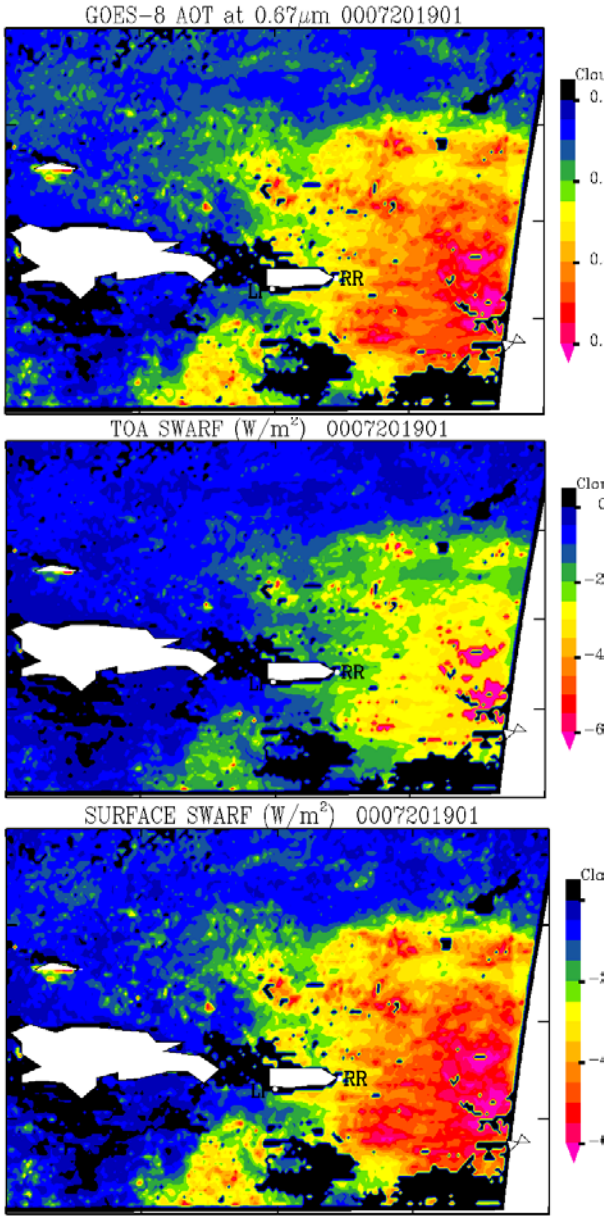

Figure 3. Geographic distribution of GOES8 AOT and calculated SWARF at TOA and surface on 1901UTC, 07/20/00.